

Optimal Treatment of Tumor Growth, using Individual Chemotherapy Doses

**Martin Dodek, Zuzana Vitková, Anton Vitko,
Jarmila Pavlovičová and Eva Miklovičová**

Institute of Robotics and Cybernetics, Faculty of Electrical Engineering and Information Technology Slovak University of Technology in Bratislava, Ilkovičova 3, 841 04 Bratislava, Slovakia, martin.dodek@stuba.sk (corresponding author), zuzana.vitkova@stuba.sk, anton.vitko@stuba.sk, jarmila.pavlovicova@stuba.sk, eva.miklovicova@stuba.sk

Abstract: This study analyzes a nonlinear model of tumor growth dynamics, describing the interactions between tumor cells, immune system cells and a chemotherapeutic drug. The primary objective is to identify a locally stable steady state corresponding to cancer remission and map its stability region in the absence of treatment. This is achieved using two approaches: first, the Lyapunov method, which provides a conservative, analytically tractable ellipsoidal region; and second, a numerical method based on iterative grid-searching, yielding a more accurate but complex and non-convex region. Additionally, we propose an optimal chemotherapy dosing protocol that minimizes the total drug amount and minimally disrupts the immune system while ensuring that the system's states move toward the natural stability region of cancer remission. To maintain remission post-treatment, a death penalty factor was applied if the terminal state fell outside the natural stability region defined by the ellipsoid inequality. Unlike other techniques in the literature, we avoid continuous drug infusion and instead consider the more practical approach of repeated chemotherapy administration as a finite sequence of individual doses (boluses). The results demonstrate that the proposed method can stabilize tumor growth across various initial conditions and induce cancer remission within a few chemotherapy doses without the need for prolonged continuously adjusted treatment.

Keywords: chemotherapy; cancer treatment; mathematical modelling; optimal control; stability region

1 Introduction

Cancer, characterized by uncontrolled cell growth and proliferation, remains a significant global health challenge [1]. The interplay of genetic, environmental, and lifestyle factors contributes to cancer's multifaceted and heterogeneous nature, necessitating innovative treatments [2]. Understanding the molecular underpinnings

of cancer has led to targeted therapies and personalized medicine. Despite these advancements, challenges persist due to tumor heterogeneity and acquired resistance [3].

Medical studies have been conducted to develop means to counteract tumor initiation, suppress its growth and proliferation, or even ensure complete remission of cancer. In the effort to enhance the treatment effectiveness, these strategies are often supported by mathematical modeling, computer simulation and control theory [4-6].

From a phenomenological perspective, tumor growth dynamics are governed by interactions with the immune system and the broader physiological environment. Numerous mechanistic mathematical models have been developed to describe tumor growth, its interactions with the immune system and responses to various cancer therapies, including chemotherapy [7-12], immunotherapy [13-15], radiotherapy [16], anti-angiogenesis [17], and their combinations [18-21]. The mechanistic models are not restricted to a specific chemotherapeutic drug or cancer subtype. Instead, they focus on the dynamics of a single solid tumor, without considering further proliferation or metastatic progression [22] [23].

Among the various control methods used for designing dosing strategies, optimal control has been the preferred approach in in-silico studies for cancer therapy development [24-29]. The methodologies in optimal control theory are primarily based on calculus of variations (Hamiltonian function) embodied in Pontryagin's maximum principle [30] [31], necessitating a solution of the corresponding two-point boundary value problem.

It is important to acknowledge the series of works by L. G. de Pillis *et al.* [26] [32], [33]. These papers analyze the geometry of state space corresponding to various mathematical models and attempt to find the conditions under which optimized time-varying chemotherapy with continuously adjustable rate can drive the system into a desirable vicinity of the chosen stable steady state.

Paper [26] provided an analysis of a mathematical model of tumor-immune interactions with chemotherapy and compared optimal control strategies for continuous administration of chemotherapy, including quadratic and linear control. The objective of the control was to reduce tumor size while minimizing the total drug administered. However, the need for sustained infusion can be viewed as a drawback since cancer can only be in a true remission when no additional chemotherapy is needed.

An interesting property of optimal control based on Pontryagin's Maximum Principle is the contrast between L_1 or L_2 type objective functions: while quadratic cost functions lead to smooth, continuous control profiles, linear cost functions produce bang-bang controls, characterized by discontinuous switching between maximum and minimum (zero) dosing rates [27] [28] [34]. This discontinuous control strategy can offer practical advantages for chemotherapy administration, as

it eliminates the need for continuous dose adjustments, simplifying implementation in clinical settings.

In [35], the model of cancer tumor growth considered both the immune system response and drug therapy. Specifically, this four-population model included tumor cells, host cells, immune cells, and drug interaction. The authors aimed to minimize only the final number of tumor cells while ensuring that the number of normal cells remained above a fixed threshold throughout the entire course of treatment. To derive the control law for continuous drug infusion, the Hamiltonian for the optimal control problem was formulated, and the solution was obtained numerically.

Besides optimal chemotherapy, another approach is based on optimal anti-angiogenesis, which can be found in the work of U. Ladzewicz [14] [15] [18] [19], [36], P. Bajger [21] and T. Ferenci [37]. More specifically, in [19], the problem of minimizing the tumor volume while combining anti-angiogenic and cytotoxic agents was addressed. The problem was formulated as an optimal control problem with free terminal time and constraints limiting the quantities of the agents to be administered. However, the considered functional involved only the terminal penalty for the tumor size, thus the full state trajectory was not optimized.

The administration problem in cancer chemotherapy was modeled as an optimal control problem of switched systems with state-dependent switching, incorporating simple bounds on the decision variables in [8].

In contrast to optimization-based approaches, as described in [38], three nonlinear controllers, namely the Lyapunov-based controller, sliding mode controller, and terminal sliding mode-based controller have been developed to regulate chemotherapy infusion. The objective of the design was to diminish and stabilize the number of brain tumor cells, sustain a safe count of healthy cells, ensure immune cells remain above a specified threshold, and restrict the amount of administered anticancer drug. To suppress chattering in the drug injection typical for sliding mode control, a smooth super-twisting control was proposed in [39].

In [20], the authors designed an optimal cancer therapy where patient-specific uncertainties were addressed using multiple model adaptive control, a technique where both the model and the controller gains are adaptively selected to optimize outcomes. The tumor growth model was linearized around its equilibrium point, and a linear quadratic controller was designed for each model in a finite set.

Similarly, robust linear controller is designed using a H_∞ methodology, based on a linearized nominal model, while taking into account the modeling uncertainties caused by the nonlinearities of the system and parametric uncertainties, was described in [40].

Concerning the stability analysis, in [24] conditions for the existence and stability of equilibrium points have been presented in both drug-free and treated scenario. Local stability of the coexisting equilibrium point was proved in terms of eigenvalue analysis of Jacobian matrix of system using the Routh–Hurwitz rule. A similar

approach for studying the local stability of steady states based on the definiteness of the Jacobian matrix was pursued in [21] [26] [29] [41]. Despite providing essential information, the region (boundary geometry) of the local stability region remained unknown.

Another problem is that all the aforementioned works assume the administration of chemotherapy in the form of continuous infusion (continuous optimal control). However, in the current medical practices, the application of a continuous drug protocol is not recommended nor convenient as it is more practical to rather administer a few discrete doses (boluses) [34] [42]. As an exception, in [43] cancer is treated by periodically administered constant doses. From the point of view of cybernetics, this is an impulse control system, where the amount and frequency of drug used can be determined using the impulse control theory. In [43], the globally stable condition for prescription of a periodic oscillatory chemotherapeutic agent was derived. The authors demonstrated the stability of the equilibrium point, the stability of the periodic oscillation of the chemotherapeutic agent, and the condition under which chemotherapy can eliminate the cancer cells and preserve the immune cells. However, a significant drawback is the assumption of constant (fixed) drug size without allowing for variable drug dosing.

The optimization and control of tumor growth dynamics share fundamental challenges with various complex control systems [44], including robotic applications [45] and telerobotic systems [46]. Moreover, hybrid control strategies like ADRC-SMC in tower cranes [47] parallel the integration of adaptive and optimal methods in cancer therapy. In telerobotic surgery and space medicine [48], handling the variability of human tissue and environmental constraints is analogous to accounting for tumor microenvironment changes. Furthermore, reinforcement learning-based adaptive control in crane systems [49] shares similarities with optimizing chemotherapy protocols.

In contrast to the referenced studies, with their methodological shortcomings and identified research gaps, this paper presents a novel approach by introducing three key innovations:

- Pulsatile (bolus-like) chemotherapy administration: Rather than assuming continuous infusion, the proposed method delivers variable discrete doses at periodic intervals, better reflecting real-world clinical practice.
- Comprehensive consideration of immune dynamics: Beyond focusing solely on tumor size, this study also incorporates the dynamics of cytotoxic lymphocytes and natural killer cells.
- Rigorous stability boundary analysis: Instead of relying on basic local stability analysis based on the Jacobian matrix's definiteness, this work employs a Lyapunov-based approach to explicitly characterize the guaranteed stability region (boundary) as an ellipsoidal inequality. By embedding this stability constraint directly into the optimization problem, the method ensures that the

terminal state remains within the natural stability region, thereby guaranteeing sustained remission following the completion of therapy.

The goals and main contributions of this study can be stated as follows:

The first goal is to identify a locally stable steady state associated with cancer remission and characterize its stability region in the absence of treatment. To meet this goal, the mathematical model of tumor growth is examined to identify steady states and classify them based on clinical interpretation and local stability. A desired steady state is then selected for further analysis. The natural stability region (region of attraction) of this state is determined using the Lyapunov approach, resulting in conservative yet analytically tractable ellipsoid inequality. This is subsequently refined through iterative grid mapping using numerical solution of differential equations to obtain a more accurate, but complex non-convex stability region. Identifying this stability region helps to define the threshold for cancer remission in the absence of chemotherapy.

The second goal is to design an optimal treatment strategy by adjusting the dosing protocol for bolus-like chemotherapy. The administration of chemotherapy is intended to guide the system's state trajectories toward the natural stability region, ensuring convergence to the desired steady state from a broad range of adverse initial conditions using only a finite sequence of discrete doses. To achieve this, a terminal-time stability penalty—expressed as an ellipsoid inequality—is incorporated into the optimization problem. This guarantees that, once the finite chemotherapy regimen concludes, the system remains stable and is naturally attracted to the remission state. By following this optimized dosing protocol, the therapeutic objective is met while minimizing the total drug dosage and reducing disruptions to the immune system.

The paper is structured as follows: Section 2.1 presents the adopted nonlinear mathematical model of the tumor growth dynamics, analyzes its steady states and their classification according to local stability. The conventional stability analysis using Lyapunov theory is presented in section 2.2. The region of natural stability for the chosen steady state is then numerically mapped in section 2.3. The design of optimal dosing protocol for chemotherapy to achieve successful treatment is addressed in section 2.4. The simulation experiments to validate the proposed methodology are presented in section 3. Conclusions are drawn in section 4.

2 Methodology

2.1 Mathematical Model of the Tumor Growth Dynamics

The model will be adopted from the work of G. Song *et al.* [10], which describes the dynamics of four state variables:

- $N(t)$ natural killer cells population
- $L(t)$ cytotoxic lymphocytes population
- $T(t)$ tumor cell population
- $u(t)$ amount of drug in the tumor site

forming the state vector $x(t) = (N(t) \ L(t) \ T(t) \ u(t))^T$

The model is defined by nonlinear ordinary differential equations (1) describing the evolution of the state variables $N(t)$, $L(t)$, and $T(t)$.

$$\begin{aligned}\dot{N}(t) &= N(t)(a(1 - bN(t)) - \alpha_1 T(t) - k_N u(t)) \\ \dot{L}(t) &= rN(t)T(t) - L(t)(\mu + \beta_1 T(t) + k_L u(t)) \\ \dot{T}(t) &= T(t)(c(1 - dT(t)) - \alpha_2 N(t) - \beta_2 L(t) - k_T u(t))\end{aligned}\tag{1}$$

Nonlinear differential equations in (1) are supplemented by linear differential equation (2) describing the dynamic relationship between the amount of the chemotherapeutic agent inside the tumor $u(t)$ and the rate of drug administration $v(t)$.

$$\dot{u}(t) = v(t) - \omega u(t)\tag{2}$$

The explanation and units of the model parameters can be found in [10].

For $t \rightarrow \infty$ and terminated treatment manifesting by $v(t) = u(t) = 0$, the state variables of model (1) approach their steady values N_0, L_0, T_0 . Given the fact that (1) is a nonlinear system, it has multiple steady states, each with a specific (or none) region of attraction. The steady states can be determined numerically as the solutions of algebraic equations emerging from (1) when assuming $\dot{N}(t) = \dot{L}(t) = \dot{T}(t) = 0$. Due to quadratic nonlinear nature of (1), the steady states are obtained as simultaneous solutions of three quadratic forms (intersection of three quadratic surfaces in three dimensions).

The Jacobian matrix $A(N_0, L_0, T_0)$ of model (1) is then given by:

$$\begin{aligned}
 A(N_0, L_0, T_0) &= \begin{pmatrix} \frac{d\dot{N}(t)}{dN(t)} & \frac{d\dot{N}(t)}{dL(t)} & \frac{d\dot{N}(t)}{dT(t)} \\ \frac{d\dot{L}(t)}{dN(t)} & \frac{d\dot{L}(t)}{dL(t)} & \frac{d\dot{L}(t)}{dT(t)} \\ \frac{d\dot{T}(t)}{dN(t)} & \frac{d\dot{T}(t)}{dL(t)} & \frac{d\dot{T}(t)}{dT(t)} \end{pmatrix}_{N(t)=N_0, L(t)=L_0, T(t)=T_0, u(t)=u_0} \\
 &= \begin{pmatrix} \alpha(1 - 2bN_0) - \alpha_1 T_0 - k_N u_0 & 0 & -\alpha_1 N_0 \\ rT_0 & -(\mu + \beta_1 T_0 + k_L u_0) & rN_0 - \beta_1 L_0 \\ -\alpha_2 T_0 & -\beta_2 T_0 & c(1 - 2dT_0) - \alpha_2 N_0 - \beta_2 L_0 - k_T u_0 \end{pmatrix} \\
 &\quad (3)
 \end{aligned}$$

The motivation for studying the properties of Jacobian matrix $A(N_0, L_0, T_0)$ is to determine the local stability of the corresponding equilibrium point based on its definiteness. If $A(N_0, L_0, T_0) < 0$ then the equilibrium point is locally stable but the properties of the attraction region are unknown.

There are four possible clinical scenarios for the steady states. The first is the Dead state, where all state variables are zero, indicating the elimination of the tumor but also the depletion of the immune system—an undesirable outcome from a clinical standpoint. The most favorable scenario is the Cured state, characterized by the complete absence of tumor cells and a sufficient presence of natural killer (N) cells. However, this state is typically unstable and cannot be sustained. The worst-case scenario is the Grown state, marked by a high tumor cell count, representing advanced-stage cancer. Therefore, the most viable option is the Coexisting state, where cancer remains in remission with a small population of T cells and an adequate number of N cells.

Considering no treatment $v(t) = u(t) = 0$, the names assigned according to clinical interpretations and coordinates of the steady states (equilibrium points) are given in Table 1. For all stationary points from Table 1, the local stability was investigated based on the definiteness of the Jacobian matrix (3).

Table 1
Names and coordinates of the steady states in the state space defined by variables N, L, T

	Stability	N_0	L_0	T_0
Dead	Unstable	0	0	0
Coexisting 1	Stable	3.1273×10^5	1.4672×10^6	8.6566×10^5
Coexisting 2	Unstable	6.5644×10^3	1.3219×10^6	9.7919×10^7
Cured	Unstable	3.1546×10^5	0	0
Grown	Stable	0	0	9.8039×10^8

Even though $T_0 = 8.6566 \times 10^5$ in the case of Coexisting state 1 is clearly much more than zero (complete remission), comparing it with $T_0 = 9.8039 \times 10^8$ in the case of Grown state means that the tumor cell population is roughly 1000 times smaller. Therefore, Coexisting state 1 seems to be the best option as it corresponds to cancer in partial remission.

2.2 Stability Analysis According to Lyapunov Approach

In this section, the Lyapunov approach will be applied to find the guaranteed stability region of the cancer remission (without the treatment) in the form of an analytically tractable ellipsoid inequality condition.

Consider a quadratic Lyapunov function $V(N, L, T)$ such that:

$$V(N, L, T) = \frac{1}{2}\lambda_1(N - N_0)^2 + \frac{1}{2}\lambda_2(L - L_0)^2 + \frac{1}{2}\lambda_3(T - T_0)^2 \quad (4)$$

where $\lambda_1 > 0$, $\lambda_2 > 0$, $\lambda_3 > 0$ are the tuning coefficients. Lyapunov function (4) then satisfies the necessary conditions $V(N, L, T) \geq 0$ and $V(N_0, L_0, T_0) = 0$.

Consider a sub-level set of a Lyapunov function $V(N, L, T)$ given by the inequality:

$$V(N, L, T) \leq 1 \quad (5)$$

For (4), the states will satisfy the ellipsoid inequality:

$$0 < \frac{1}{2}\lambda_1(N - N_0)^2 + \frac{1}{2}\lambda_2(L - L_0)^2 + \frac{1}{2}\lambda_3(T - T_0)^2 \leq 1 \quad (6)$$

Taking the time derivative $\dot{V}(N, L, T)$ of (4) results in:

$$\dot{V}(N, L, T) = \lambda_1(N - N_0)\dot{N}(t) + \lambda_2(L - L_0)\dot{L}(t) + \lambda_3(T - T_0)\dot{T}(t) \quad (7)$$

Notice that $\dot{V}(N_0, L_0, T_0) = 0$

Substituting the model equations (1) into (7) yields:

$$\dot{V}(N, L, T) = \lambda_1(N - N_0)(N(a(1 - bN) - \alpha_1T - k_N u)) + \lambda_2(L - L_0)(rNT - L(\mu + \beta_1T + k_L u)) + \lambda_3(T - T_0)(T(c(1 - dT) - \alpha_2N - \beta_2L - k_T u)) \quad (8)$$

Considering no therapy $u(t) = 0$ results in:

$$\dot{V}(N, L, T) = \lambda_1 N(-N^2 ab + N(a - \alpha_1 T + abN_0) - N_0(a - \alpha_1 T)) + \lambda_2(-L^2(\mu + \beta_1 T) + L(rNT + L_0(\mu + \beta_1 T)) - L_0 rNT) + \lambda_3 T(-T^2 cd + T(c - \alpha_2 N - \beta_2 L + cdT_0) - T_0(c - \alpha_2 N - \beta_2 L)) \quad (9)$$

Clearly, for arbitrary unbounded N, L, T , the time derivative $\dot{V}(N, L, T)$ in (9) does not satisfy the stability condition $\dot{V}(N, L, T) < 0$, hence the system is not globally stable at N_0, L_0, T_0 .

Therefore, the goal is to determine whether for N, L, T satisfying inequality (6) for given $\lambda_1, \lambda_2, \lambda_3$, the time derivative $\dot{V}(N, L, T)$ satisfies $\dot{V}(N, L, T) < 0$. Finding $\lambda_1,$

λ_2, λ_3 such that $\dot{V}(N, L, T) < 0$ subject to constraint $V(N, L, T) \leq 1$ means that we found a finite region of stability of the equilibrium N_0, L_0, T_0 .

Unfortunately, verifying the boundedness of $\dot{V}(N, L, T)$ in the region constrained by ellipsoid $V(N, L, T) \leq 1$ cannot be done analytically. Instead, a constrained numerical maximization of $\dot{V}(N, L, T)$ must be performed such that:

$$N^*, L^*, T^* = \arg \max \left(\dot{V}(N, L, T) \right) \text{ subj. to } V(N, L, T) \leq 1 \quad (10)$$

The constraint function $g(N, L, T)$ is:

$$g(N, L, T) = \frac{1}{2}\lambda_1(N - N_0)^2 + \frac{1}{2}\lambda_2(L - L_0)^2 + \frac{1}{2}\lambda_3(T - T_0)^2 - 1 \leq 0 \quad (11)$$

The sufficient stability condition then gets

$$\dot{V}(N^*, L^*, T^*) = 0, N^* = N_0, L^* = L_0, T^* = T_0 \quad (12)$$

If (12) is satisfied, then for an arbitrary state N, L, T lying inside the region given by $V(N, L, T) \leq 1$, the state trajectory will converge to N_0, L_0, T_0 .

To efficiently solve the constrained maximization problem (10), it is necessary to find the gradient of $\dot{V}(N, L, T)$ and gradient of the constraint function $g(N, L, T)$.

The partial derivatives of $\dot{V}(N, L, T)$ can be derived according to (8) as:

$$\begin{aligned} \frac{\partial \dot{V}(N, L, T)}{\partial N} &= \lambda_1(-3N^2ab + (2N - N_0)(a - \alpha_1T) + 2NabN_0) + \lambda_2rT(L - L_0) + \lambda_3\alpha_2T(-T + T_0) \\ \frac{\partial \dot{V}(N, L, T)}{\partial L} &= \lambda_2(-(2L - L_0)(\mu + \beta_1T) + rNT) + \lambda_3T\beta_2(-T + T_0) \end{aligned} \quad (13)$$

$$\frac{\partial \dot{V}(N, L, T)}{\partial T} = \lambda_1\alpha_1N(-N + N_0) + \lambda_2(-\beta_1L^2 + L(rN + L_0\beta_1) - L_0rN) + \lambda_3(-3T^2cd + 2TcdT_0 + (2T - T_0)(c - \alpha_2N - \beta_2L))$$

The partial derivatives of $g(N, L, T)$ can be derived according to (11) as:

$$\frac{\partial g(N, L, T)}{\partial N} = \lambda_1(N - N_0), \frac{\partial g(N, L, T)}{\partial L} = \lambda_2(L - L_0), \frac{\partial g(N, L, T)}{\partial T} = \lambda_3(T - T_0) \quad (14)$$

Then, numerical optimization methods based on Karush–Kuhn–Tucker conditions, such as interior point methods, can be used.

Considering coefficients $\lambda_1 = 0.05 \times 10^{-8}$, $\lambda_2 = 0.27 \times 10^{-8}$, $\lambda_3 = 0.0300 \times 10^{-8}$ in Lyapunov function (4), which were adjusted in attempt to maximize the volume of the corresponding ellipsoid, the maximization problem (10) was solved while satisfying (12), thus validating the negative value of $\dot{V}(N, L, T)$.

The resulting region of stability defined by an ellipsoid given by (6) is visualized in Figure 1. This figure demonstrates that the region of stability is relatively small as it allows only a few percent variations of the state variables, taken relatively with respect to the considered steady state, for stability (attraction) to be ensured.

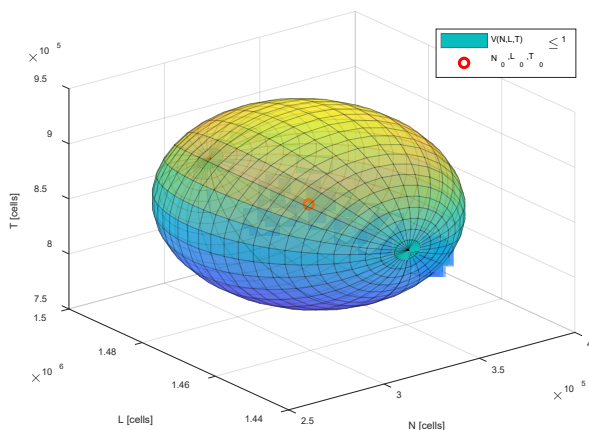


Figure 1

Natural region of stability of cancer remission obtained using the Lyapunov approach

However, it is important to note that this ellipsoid does not represent the full stability region (complete stability boundary) since there might exist different coefficients $\lambda_1, \lambda_2, \lambda_3$ to obtain different stability regions. Besides that, the actual stability region is not likely to be an ellipsoid but rather a more complex shape asymmetrical with respect to the steady state N_0, L_0, T_0 . From this perspective, the Lyapunov approach can be considered quite conservative, but computationally tractable.

2.3 Numerical Mapping of Natural Stability Region

Due to limitations of the Lyapunov approach, the region of natural stability of cancer remission will be mapped by numerically integrating the nonlinear model (1) for the total time of $t_f = 500$ days considering variety of initial conditions $N(0), L(0), T(0)$ arranged in a three-dimensional grid and by subsequent checking for the convergence to N_0, L_0, T_0 .

In detail, the three-dimensional grid of the testing initial conditions $N(0), L(0), T(0)$ was spaced linearly with the dimensions $100 \times 100 \times 100$ implying the total of 10^6 different trajectories while considering the following intervals $0 \leq N(0) \leq 10^6, 0 \leq L(0) \leq 10^7, 0 \leq T(0) \leq 10^9$. The individual initial conditions $N(0), L(0), T(0)$ from this finite set were classified based on the convergence of the corresponding state responses $N(t), L(t), T(t)$ to the equilibrium N_0, L_0, T_0 according to Lyapunov stability condition (6) defining the ellipsoid inequality $\frac{1}{2}\lambda_1(N(t_f) - N_0)^2 + \frac{1}{2}\lambda_2(L(t_f) - L_0)^2 + \frac{1}{2}\lambda_3(T(t_f) - T_0)^2 \leq 1$. The obtained stability region is then visualized in Figure 2. For all initial states $N(0), L(0), T(0)$ located inside this region, the state trajectories will converge to the Coexisting state 1 without the treatment.

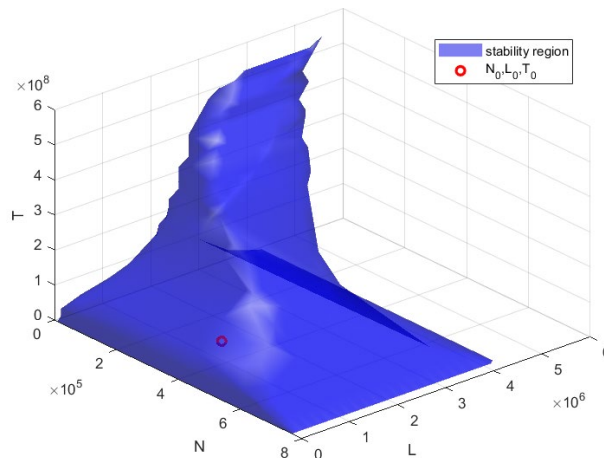


Figure 2

Numerically mapped natural region of stability of cancer remission

The region of natural stability forms a three-dimensional nonconvex hull. One can notice that its base, where $T(0)$ is very small, has the largest area of stability in the positive N-L plane. This suggests that if the tumor is sufficiently small, the immune system doesn't need to be in an ideal (specific) condition to inhibit further tumor growth.

As tumor cells emerge and proliferate, the area of stability in the N-L plane progressively contracts in both dimensions. In other words, the conditions for state variables N and L of the immune system become increasingly stringent, leading to the formation of a pyramidal hull-shaped region of stability. This pyramidal shape arises because reaching certain critical thresholds of N and L cell quantities, which become tighter and stricter with an increasing tumor size, creates more favorable conditions for tumor growth and proliferation.

Comparing Figures 1 and 2, it is evident that the numerically mapped stability region is much larger than the conservative ellipsoid, particularly in the T state, where the stability region spans multiple magnitudes. Besides that, there can be observed a strong asymmetry of the stability region with respect to the equilibrium N_0, L_0, T_0 .

A significant drawback of the numerical mapping is its computational complexity associated with repetitive numerical solution of differential equations across a dense three-dimensional grid of the testing initial conditions (10^6 in total). Another disadvantage is that the obtained stability region, is not a convex hull and thus, cannot be expressed using a set of linear inequalities and further refined in the therapy design.

2.4 Optimization of Chemotherapy Doses

The aim of the chemotherapy dosing schedule design is to drive the system state from the initial state $N(0), L(0), T(0)$ optimally to the natural stability region of the Coexisting state 1 defined by the triplet N_0, L_0, T_0 (see Table 1) representing the cancer in remission. After guiding the states to this stability region, the chemotherapy can be completely stopped and the states are naturally attracted to the Coexisting state 1.

Assume that the therapy consists of administering a finite sequence of n_d individual (discrete) doses (boluses) of chemotherapy in the form of short and uniformly spaced pulses periodically with the period of T_D days.

Each of these n_d doses constitutes a decision variable to be determined. The doses will be modelled as a rectangular pulse of the administration rate $v(t)$, which has the duration of $0.1 \times T_D$ and the amplitude of $D_i \times \frac{10}{T_D}$ in order to ensure that the area under the curve of the corresponding pulse is equal to D_i .

The optimization problem will consider a decision vector D of n_d positive doses of chemotherapy constituting the input administration rate (control) signal $v(t)$ as

$$v(t) = \begin{cases} D_i \times \frac{10}{T_D} & \text{if } 0 \leq t - (i-1)T_D \leq \frac{T_D}{10} \text{ for } i = 1, 2 \dots n_d, \\ 0 & \text{otherwise} \end{cases}$$

$$D = (D_1 \quad D_2 \quad D_3 \quad \dots \quad D_{n_d})^T \quad (15)$$

which will drive the system state towards the Coexisting state 1 following the optimal trajectory, while the total amount of administered chemotherapy will be minimal.

To this end, we define an integral quadratic criterion:

$$J(D) = \int_0^{t_f} [w_N(N(t, D) - N_0)^2 + w_L(L(t, D) - L_0)^2 + w_T(T(t, D) - T_0)^2 + u^2(t, D)] dt \quad (16)$$

where t_f is the optimization horizon related to the overall treatment duration, N_0, L_0, T_0 are the coordinates of the Coexisting state 1, and $w_N > 0, w_L > 0, w_T > 0$, are the weighting coefficients.

The choice of the multicriterial integral criterion (16), which includes individual quadratic penalty terms for all state variables, is motivated by the goal of achieving a therapy that not only reduces the tumor size at the terminal time but also minimizes fluctuations in N and L cells during the treatment to preserve (minimally disturb) the immune system. Additionally, by penalizing the area under the curve of the drug amount at the tumor site u , the total chemotherapy dosage is reduced, thereby minimizing side effects on healthy cells and reducing the overall cost of therapy.

To achieve therapy optimality, criterion (16) needs to be minimized with respect to vector D , while adhering to the constraints imposed by the model's differential equations (1) and the non-negativity of the doses such that $D \geq 0$. Dynamic optimization problems are usually approached by Bellman's dynamic programming or Pontryagin's maximum principle [30] [31]. However, these standard strategies are primarily suited for applications where the control signal $v(t)$ is continuous or piecewise constant (e.g., infusion), which does not align with the chemotherapy dosing comprised of individual doses (boluses). Therefore, the problem needs to be addressed in the impulsive system framework [50] [51].

Given that our problem is finite-dimensional and integral (16) cannot be solved analytically, we opt for a numerical optimization approach. In this context, we replace the integral criterion (16) with the summation criterion (17) representing the nonlinear least-squares problem. The state trajectories $N(iT_s, D)$, $L(iT_s, D)$, $T(iT_s, D)$, $u(iT_s, D)$ are obtained by the numerical integration of (1) using the fourth order Runge-Kutta method considering T_s is the step of the numerical integration [52].

$$J(D) = \sum_{i=1}^{t_f/T_s} [w_N(N(iT_s, D) - N_0)^2 + w_L(L(iT_s, D) - L_0)^2 + w_T(T(iT_s, D) - T_0)^2 + u(iT_s, D)^2] \quad (17)$$

The weighting coefficients w_N , w_L , w_T , need to be adjusted empirically to ensure that all four penalties in (17) have roughly similar magnitudes. By maintaining similar magnitudes across penalties, we aim to achieve a balanced optimization process that appropriately considers the importance of each component in achieving the desired therapeutic outcome.

Despite the finite optimization horizon t_f (finite terminal time) in (17), long-term cancer remission after completing the therapy can be ensured. This would imply that the tumor will not eventually regrow if the state vector at the terminal time is located within the natural region of stability of the coexisting state.

Therefore, an additional death penalty term will be added to $J(D)$ to implement soft constraint. A hard constraint cannot be applied because the relationship between the doses D and the terminal state $x(t_f)$ is unknown. The soft constraint penalty based on the value of Lyapunov function (4) and the ellipsoid condition (6) will be defined discontinuously as:

$$S = \begin{cases} 0 & \text{if } V(N(t_f), L(t_f), T(t_f)) \leq 1 \\ w_s (V(N(t_f), L(t_f), T(t_f)) - 1) & \text{if } V(N(t_f), L(t_f), T(t_f)) > 1 \end{cases} \quad (18)$$

where $w_s > 0$ is a very large number.

Since D_i represent positive quantities of chemotherapy to be administered, the additional constraints on vector (15) are imposed as $D \geq \mathbf{0}$ and $D \leq \mathbf{1}D_{max}$, where the maximal chemotherapy dose is $D_{max} = 5$ IU. Constraint D_{max} can be

interpreted as the maximal admissible chemotherapy dose that will not kill the patient. The final optimization problem can be stated as:

$$\begin{aligned} \min_D \sum_{i=1}^{\frac{t_f}{T_s}} & [w_N(N(iT_s, D) - N_0)^2 + w_L(L(iT_s, D) - L_0)^2 + w_T(T(iT_s, D) - T_0)^2 \\ & + u(iT_s, D)^2] + \begin{cases} 0 & \text{if } V(N(t_f), L(t_f), T(t_f)) \leq 1 \\ w_s(V(N(t_f), L(t_f), T(t_f)) - 1) & \text{otherwise} \end{cases} \\ \text{subj. to } D & \geq \mathbf{0}, D \leq \mathbf{1}D_{max} \\ \dot{N}(t) &= N(t)(a(1 - bN(t)) - \alpha_1T(t) - k_Nu(t)) \quad (19) \\ \dot{L}(t) &= rN(t)T(t) - L(t)(\mu + \beta_1T(t) + k_Lu(t)) \\ \dot{T}(t) &= T(t)(c(1 - dT(t)) - \alpha_2N(t) - \beta_2L(t) - k_Tu(t)) \\ \dot{u}(t) &= v(t) - \omega u(t) \\ v(t) &= \begin{cases} D_i \times \frac{10}{T_D} & \text{if } 0 \leq t - (i-1)T_D \leq \frac{T_D}{10} \text{ for } i = 1, 2 \dots n_D \\ 0 & \text{otherwise} \end{cases} \end{aligned}$$

To obtain vector D that solves the optimization problem (19), numeric optimization implemented in the *fmincon* function of Matlab optimization toolbox [53] was used. This function implements some of the well-known interior-point methods for constrained numeric optimization [54] [55].

Interior-point algorithms form a group of optimization techniques that navigate through the interior of the feasible domain rather than along its boundaries. These methods incorporate a barrier term—often logarithmic in form—into the objective function to discourage solutions from approaching constraint edges too closely. A key concept in these approaches is the "central path," which traces the progression of solutions to the barrier-modified problem as the influence of the barrier term diminishes. This path ultimately leads to the solution that fulfills both the primal and dual optimality criteria, typically characterized by the Karush–Kuhn–Tucker (KKT) conditions. In the context of nonlinear least-squares problems, such as (19), where analytical derivatives are not available, the *fmincon* solver estimates gradients using finite differences and approximates the Hessian through a quasi-Newton strategy.

3 Results

In this section, we will perform simulation experiments to validate the proposed methodology. Let the optimization horizon be $t_f = 100$ days, the time step of numerical integration $T_s = 1/100$ day, the number of doses $n_D = 5$, and the dosing

period $T_D = 14$ days. The weights in (19) were chosen as $w_N = 10^{-10}$, $w_L = 10^{-12}$, $w_T = 10^{-14}$, $w_s = 10^{16}$.

Consider the initial state $N(0) = 0.5 N_0$, $L(0) = 0.5 L_0$, $T(0) = 1.0 \times 10^8$, which leads to the grown state in the absence of chemotherapy since it is outside the natural stability region (see Figure 2). This implies that treatment is necessary to ensure remission. The optimal chemotherapy dosing protocol was determined as $D = (2.2918 \ 1.1097 \ 2.0709 \ 1.6448 \ 0.7855)^T$.

The corresponding state trajectory is shown in Figure 3 and the evolutions of the states are shown in Figure 4, demonstrating that the states are converging towards the desired Coexisting state 1, hence the designed therapy ensures the remission of cancer.

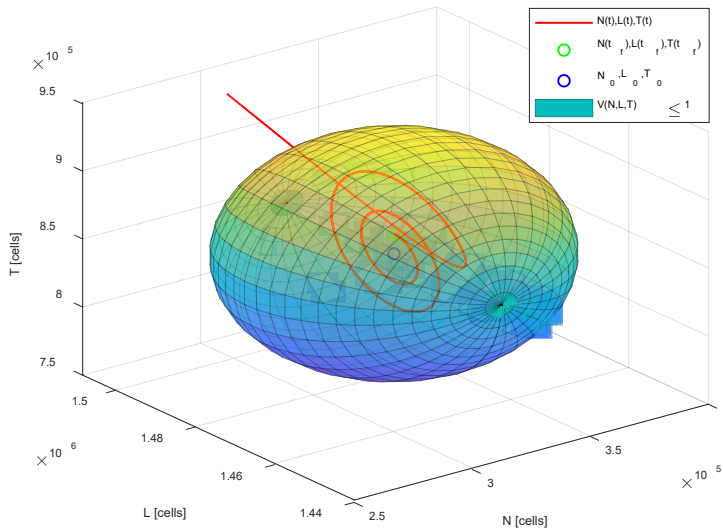


Figure 3

State trajectory of the state variables N, L, T and stability region for scenario 1

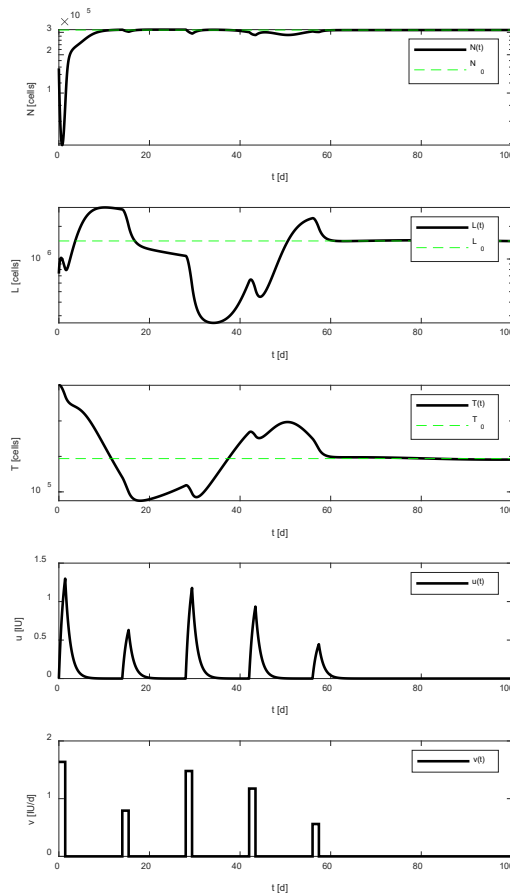


Figure 4

Evolution of the state variables N , L , T , and u in time according to input v for scenario 1

Now consider an even more demanding initial condition $N(0) = 0.1 N_0$, $L(0) = 0.1 L_0$, $T(0) = 2.0 \times 10^8$ in which the immune system is significantly weakened and tumor is larger. The optimal chemotherapy dosing protocol was determined as $D = (3.7850 \ 1.9477 \ 3.3067 \ 1.9020 \ 0.7604)^T$.

The corresponding state trajectory is shown in Figure 5 and the evolutions of the states are shown in Figure 6, demonstrating that the states are converging towards the desired Coexisting state 1, so the treatment can be considered successful.

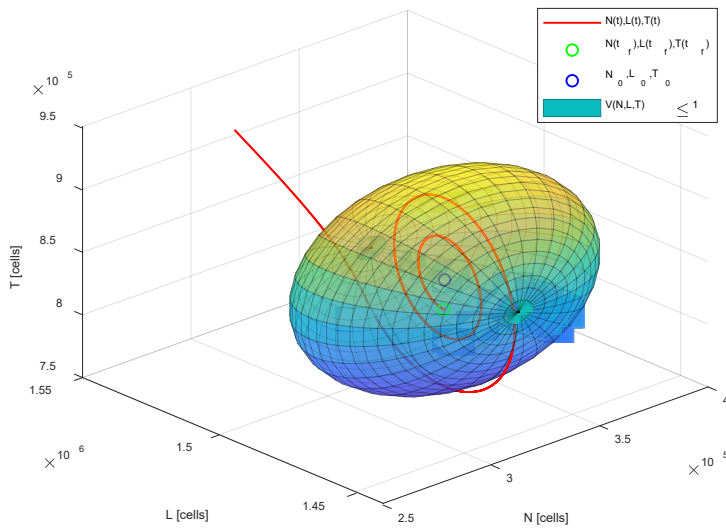


Figure 5

State trajectory of the state variables N , L , T and stability region for scenario 2

The state trajectories in Figures 3 and 5, document that the terminal state $N(t_f)$, $L(t_f)$, $T(t_f)$ lies inside the stability region bounded by ellipsoid from Figure 1. Therefore, the future convergence of the states to the steady state N_0 , L_0 , T_0 is guaranteed due to the natural attraction (stability) despite the treatment is completed.

The Matlab source code associated with this paper is publicly available at Github repository: <https://github.com/dodekm/Optimal-Treatment-of-Tumor-Growth-Using-Individual-Doses-of-Chemotherapy>

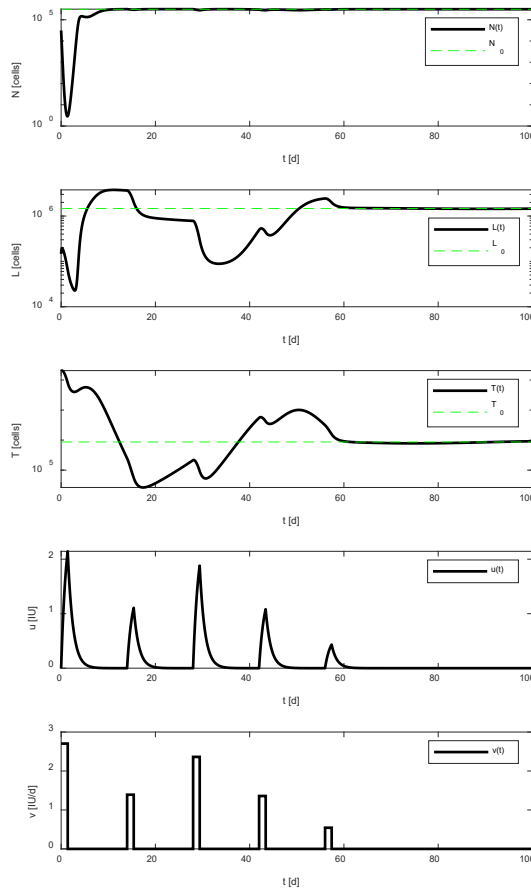


Figure 6

Evolution of the state variables N , L , T , and u in time according to input v for scenario 2

Conclusions

This study presented an insight into phenomenologic (mechanistic) tumor growth modelling, by identifying a locally stable steady-state associated with cancer remission, determining its stability region and proposing an optimal chemotherapy dosing protocol, based on individual boluses.

A key contribution of this work is the mapping of the natural stability region, using two different approaches. The Lyapunov-based approach provided a conservative yet computationally feasible estimate of the stability region, while the numerical iterative grid searching offered a more precise but computationally intensive mapping. The numerically mapped stability region was significantly larger than the ellipsoid, indicating that the Lyapunov approach is conservative but useful for defining the boundaries of remission by a single inequality. Furthermore, the

numerical mapping revealed a highly asymmetric and nonconvex stability region, hindering its description by a system of linear inequalities.

To determine the optimal dosing protocol, we considered a summation quadratic criterion over a finite horizon, which can be seen as a nonlinear least squares problem, and facilitated the numerical optimization with the state responses obtained by the numerical solution of model differential equations.

Biologically, optimizing the dosing protocol mitigates the disruptions to the immune system and minimizes the administered chemotherapy, thereby reducing its negative side effects on healthy cells. From a cybernetic perspective, systematic design of the dosing protocol provides stabilization by guiding the state towards the natural stability region, effectively enabling cancer remission in adverse conditions.

Another striking feature is that, unlike conventional continuous infusion methods, which often assume constant or continuously varying drug administration, the approach proposed in this study focuses on discrete boluses. This not only ensures remission while minimizing drug administration and immune system disruption but also aligns better with real-world clinical practices, where bolus dosing is more practical and widely used.

The topology of clinical application of the proposed optimizer of chemotherapy doses is outlined in Figure 7.

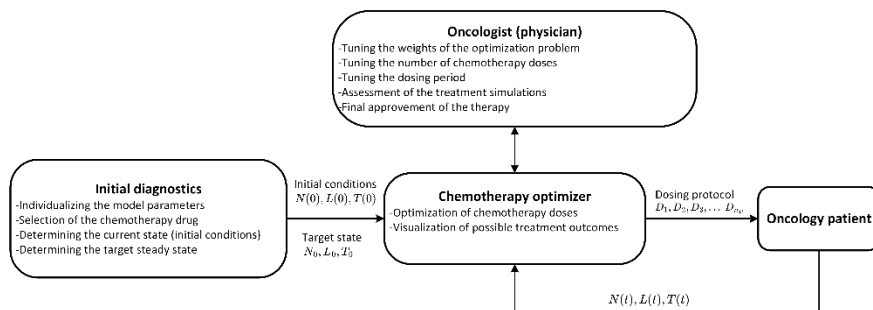


Figure 7

Topology of clinical application of the proposed optimizer of chemotherapy doses

The simulation results confirmed the practical applicability of the proposed approach by demonstrating that remission could be achieved under a variety of adverse initial conditions. The first simulation scenario, where the immune system was relatively strong, required a moderate chemotherapy dose sequence, which successfully guided the system to the natural stability region. In contrast, a second scenario, with a weakened immune response and larger tumor, required a higher total chemotherapy dosage but still converged to remission. Importantly, in both cases, the final state remained within the stability region, ensuring that remission was maintained without requiring sustained treatment.

Unlike prior works that focus on minimizing tumor size and drug quantity, our methodology explicitly incorporates cytotoxic lymphocytes and natural killer cell populations into the optimization problem.

The chemotherapy dosing protocol designed in this study is noteworthy for its ability to transition the system into remission within a finite number of treatment cycles. By incorporating a terminal-state stability constraint into the optimization framework, the method ensures that the final system state resides within the natural stability region. The inclusion of a death penalty in the optimization function effectively prevents scenarios where remission is achieved temporarily but lacks long-term stability.

While the results are promising, certain limitations should be acknowledged.

First, the model assumes a single solid tumor and does not account for metastasis. Future studies should explore extending the model, to incorporate metastatic spread and adaptive resistance mechanisms. Second, the computational complexity of the numerical stability mapping, remains a challenge. Third, *in vivo* and clinical validation are necessary to confirm the real-world effectiveness of the proposed dosing strategy. Although the mathematical model is grounded in biologically relevant principles, experimental validation would provide essential insights into the feasibility and safety of the proposed approach. And finally, a limitation arises from the formulation of the nonlinear least square's optimization problem, as it introduces the possibility of multiple local extrema. This, in turn, increases the risk of the optimization algorithm converging to a suboptimal local extremum rather than the global optimum. One potential solution is to employ global optimization techniques, such as stochastic methods (e.g., simulated annealing, genetic algorithms).

Acknowledgement

The research is supported by the grant VEGA 1/0229/24 Advanced methods of modeling, identification and control of biosystems, granted by the Ministry of education, science, development, and sport of the Slovak republic.

References

- [1] D. Hanahan and R. A. Weinberg, "Hallmarks of Cancer: The Next Generation," *Cell*, Vol. 144, No. 5, pp. 646-674, Mar. 2011, doi: 10.1016/j.cell.2011.02.013
- [2] A. V Biankin *et al.*, "Pancreatic cancer genomes reveal aberrations in axon guidance pathway genes," *Nature*, Vol. 491, No. 7424, pp. 399-405, 2012, doi: 10.1038/nature11547
- [3] L. A. Garraway and P. A. Jänne, "Circumventing Cancer Drug Resistance in the Era of Personalized Medicine," *Cancer Discov*, Vol. 2, No. 3, pp. 214-226, Mar. 2012, doi: 10.1158/2159-8290.CD-12-0012

- [4] J. Sápi, D. A. Drexler, and L. Kovács, “Potential Benefits of Discrete-Time Controller-based Treatments over Protocol-based Cancer Therapies,” *Acta Polytechnica Hungarica*, Vol. 14, No. 1, pp. 11-23, 2017, doi: 10.12700/APH.14.1.2017.1.2
- [5] M. F. Dömény, M. Puskás, L. Kovács, T. T. Mac, and D. A. Drexler, “Detecting critical supervision intervals during in silico chemotherapy treatments,” *Acta Polytechnica Hungarica*, Vol. 21, No. 9, pp. 247-261, 2024
- [6] L. Kovács and G. Eigner, “Tensor Product Model Transformation based Parallel Distributed Control of Tumor Growth,” *Acta Polytechnica Hungarica*, Vol. 15, No. 3, pp. 101-123, 2018, doi: 10.12700/APH.15.3.2018.3.7
- [7] F. S. Borges *et al.*, “Model for tumour growth with treatment by continuous and pulsed chemotherapy,” *Biosystems*, Vol. 116, pp. 43-48, 2014, doi: <https://doi.org/10.1016/j.biosystems.2013.12.001>
- [8] X. Wu, Y. Hou, and K. Zhang, “Switched system optimal control approach for drug administration in cancer chemotherapy,” *Biomed Signal Process Control*, Vol. 75, p. 103575, 2022, doi: <https://doi.org/10.1016/j.bspc.2022.103575>
- [9] X. Wu, Q. Liu, K. Zhang, M. Cheng, and X. Xin, “Optimal switching control for drug therapy process in cancer chemotherapy,” *Eur J Control*, Vol. 42, pp. 49-58, 2018, doi: <https://doi.org/10.1016/j.ejcon.2018.02.004>
- [10] G. Song, G. Liang, T. Tian, and X. Zhang, “Mathematical Modeling and Analysis of Tumor Chemotherapy,” *Symmetry (Basel)*, Vol. 14, No. 4, 2022, doi: 10.3390/sym14040704
- [11] P. Qods, J. Arkat, and Y. Batmani, “Optimal administration strategy in chemotherapy regimens using multi-drug cell-cycle specific tumor growth models,” *Biomed Signal Process Control*, Vol. 86, p. 105221, 2023, doi: <https://doi.org/10.1016/j.bspc.2023.105221>
- [12] M. Engelhart, D. Lebiez, and S. Sager, “Optimal control for selected cancer chemotherapy ODE models: A view on the potential of optimal schedules and choice of objective function,” *Math Biosci*, Vol. 229, No. 1, pp. 123-134, 2011, doi: <https://doi.org/10.1016/j.mbs.2010.11.007>
- [13] N. Sharifi, S. Ozgoli, and A. Ramezani, “Multiple model predictive control for optimal drug administration of mixed immunotherapy and chemotherapy of tumours,” *Comput Methods Programs Biomed*, Vol. 144, pp. 13-19, 2017, doi: <https://doi.org/10.1016/j.cmpb.2017.03.012>
- [14] U. Ledzewicz and H. Schättler, “On the optimal control problem for a model of the synergy of chemo- and immunotherapy,” *Optim Control Appl Methods*, Vol. 45, No. 2, pp. 575-593, Mar. 2024, doi: <https://doi.org/10.1002/oca.3016>

-
- [15] U. Ledzewicz, H. Maurer, and H. Schättler, “Bang-bang optimal controls for a mathematical model of chemo- and immunotherapy in cancer,” *Discrete and Continuous Dynamical Systems - B*, Vol. 29, No. 3, pp. 1481-1500, 2024, doi: 10.3934/dcdsb.2023141
- [16] Y. Watanabe, E. L. Dahlman, K. Z. Leder, and S. K. Hui, “A mathematical model of tumor growth and its response to single irradiation,” *Theor Biol Med Model*, Vol. 13, No. 1, p. 6, 2016, doi: 10.1186/s12976-016-0032-7
- [17] H. Schättler, U. Ledzewicz, and B. Cardwell, “Robustness of optimal controls for a class of mathematical models for tumor anti-angiogenesis,” *Mathematical Biosciences and Engineering*, Vol. 8, No. 2, pp. 355-369, 2011, doi: 10.3934/mbe.2011.8.355
- [18] U. Ledzewicz and H. Schättler, “Combination of antiangiogenic treatment with chemotherapy as a multi-input optimal control problem,” *Math Methods Appl Sci*, Vol. 45, No. 5, pp. 3058-3082, Mar. 2022, doi: <https://doi.org/10.1002/mma.7977>
- [19] U. Ledzewicz, H. Maurer, and H. Schättler, “Optimal and suboptimal protocols for a mathematical model for tumor anti-angiogenesis in combination with chemotherapy,” *Mathematical Biosciences and Engineering*, Vol. 8, No. 2, pp. 307-323, 2011, doi: 10.3934/mbe.2011.8.307
- [20] F. F. Teles and J. M. Lemos, “Cancer therapy optimization based on multiple model adaptive control,” *Biomed Signal Process Control*, Vol. 48, pp. 255-264, 2019, doi: <https://doi.org/10.1016/j.bspc.2018.09.016>
- [21] P. Bajger, M. Bodzioch, and U. Foryś, “Numerical optimisation of chemotherapy dosage under antiangiogenic treatment in the presence of drug resistance,” *Math Methods Appl Sci*, Vol. 43, No. 18, pp. 10671-10689, Dec. 2020, doi: <https://doi.org/10.1002/mma.6958>
- [22] J. S. Lowengrub *et al.*, “Nonlinear modelling of cancer: bridging the gap between cells and tumours,” *Nonlinearity*, Vol. 23, No. 1, Dec. 2009, doi: 10.1088/0951-7715/23/1/R01
- [23] A. Yin, D. J. A. R. Moes, J. G. C. van Hasselt, J. J. Swen, and H.-J. Guchelaar, “A Review of Mathematical Models for Tumor Dynamics and Treatment Resistance Evolution of Solid Tumors,” *Pharmacometrics & Systems Pharmacology*, Vol. 8, No. 10, pp. 720-737, 2019, doi: <https://doi.org/10.1002/psp4.12450>
- [24] T. Dinku, B. Kumsa, J. Rana, and A. Srinivasan, “A Mathematical Model of Tumor-Immune and Host Cells Interactions with Chemotherapy and Optimal Control,” *Journal of Mathematics*, Vol. 2024, No. 1, p. 3395825, Jan. 2024, doi: <https://doi.org/10.1155/2024/3395825>

- [25] S. Sabir, N. Raissi, and M. Serhani, "Chemotherapy and Immunotherapy for Tumors: A Study of Quadratic Optimal Control," *Int J Appl Comput Math*, Vol. 6, No. 3, p. 81, 2020, doi: 10.1007/s40819-020-00838-x
- [26] L. G. de Pillis *et al.*, "Chemotherapy for tumors: An analysis of the dynamics and a study of quadratic and linear optimal controls," *Math Biosci*, Vol. 209, No. 1, pp. 292-315, 2007, doi: <https://doi.org/10.1016/j.mbs.2006.05.003>
- [27] G. Haddad, A. Kebir, N. Raissi, A. Bouhali, and S. Ben Miled, "Optimal control model of tumor treatment in the context of cancer stem cell," *Mathematical Biosciences and Engineering*, Vol. 19, No. 5, pp. 4627-4642, 2022, doi: 10.3934/mbe.2022214
- [28] M. Dassow, S. Djouadi, and K. Moussa, "Optimal Control of a Tumor-Immune System with a Modified Stepanova Cancer Model," *IFAC-PapersOnLine*, Vol. 54, No. 15, pp. 227-232, 2021, doi: <https://doi.org/10.1016/j.ifacol.2021.10.260>
- [29] F. A. Rihan, S. Lakshmanan, and H. Maurer, "Optimal control of tumour-immune model with time-delay and immuno-chemotherapy," *Appl Math Comput*, Vol. 353, pp. 147-165, 2019, doi: <https://doi.org/10.1016/j.amc.2019.02.002>
- [30] L. R. and M.-P. S. and G.-S. D. Hernández-Lerma Onésimo and Laura-Guarachi, *An Introduction to Optimal Control Theory: The Dynamic Programming Approach*. Cham: Springer International Publishing, 2023, doi: 10.1007/978-3-031-21139-3
- [31] L. M. Hocking, *Optimal Control An Introduction to the Theory with Applications*. Oxford University Press, 1991, doi: 10.1093/oso/9780198596752.001.0001
- [32] L. G. de Pillis and A. E. Radunskaya, "Modeling Tumor-Immune Dynamics," in *Mathematical Models of Tumor-Immune System Dynamics*, A. Eladdadi, P. Kim, and D. Mallet, Eds., New York, NY: Springer New York, 2014, pp. 59-108
- [33] L. G. de Pillis, A. Eladdadi, and A. E. Radunskaya, "Modeling cancer-immune responses to therapy," *J Pharmacokinet Pharmacodyn*, Vol. 41, No. 5, pp. 461-478, 2014, doi: 10.1007/s10928-014-9386-9
- [34] P. L. Tan, H. Maurer, J. Kanesan, and J. H. Chuah, "Optimal Control of Cancer Chemotherapy with Delays and State Constraints," *J Optim Theory Appl*, Vol. 194, No. 3, pp. 749-770, 2022, doi: 10.1007/s10957-022-02046-7
- [35] L. G. De Pillis and A. Radunskaya, "A Mathematical Tumor Model with Immune Resistance and Drug Therapy: An Optimal Control Approach," *Journal of Theoretical Medicine*, Vol. 3, p. 318436, 2001, doi: 10.1080/10273660108833067

-
- [36] U. Ledzewicz and H. Schättler, “The Structure of Optimal Protocols for a Mathematical Model of Chemotherapy with Antiangiogenic Effects,” *SIAM J Control Optim*, Vol. 60, No. 2, pp. 1092-1116, 2022, doi: 10.1137/21M1395326
- [37] T. Ferenci, J. Sápi, and L. Kovács, “Modelling Tumor Growth Under Angiogenesis Inhibition with Mixed-effects Models,” *Acta Polytechnica Hungarica*, Vol. 14, No. 1, pp. 221-234, 2017, doi: 10.12700/APH.14.1.2017.1.15
- [38] M. Zubair, I. Ahmad, Y. Islam, and A. Islam, “Lyapunov based nonlinear controllers for the chemotherapy of brain tumor,” *Biomed Signal Process Control*, Vol. 68, p. 102804, 2021, doi: <https://doi.org/10.1016/j.bspc.2021.102804>
- [39] K. Rsetam, M. Al-Rawi, Z. Cao, A. Alsadoon, and L. Wang, “Model based smooth super-twisting control of cancer chemotherapy treatment,” *Comput Biol Med*, Vol. 169, p. 107957, 2024, doi: <https://doi.org/10.1016/j.compbimed.2024.107957>
- [40] L. Kovács *et al.*, “Model-based angiogenic inhibition of tumor growth using modern robust control method,” *Comput Methods Programs Biomed*, Vol. 114, No. 3, pp. e98-e110, 2014, doi: <https://doi.org/10.1016/j.cmpb.2014.01.002>
- [41] Y. D. Jeong, K. S. Kim, Y. Roh, S. Choi, S. Iwami, and I. H. Jung, “Optimal Feedback Control of Cancer Chemotherapy Using Hamilton–Jacobi–Bellman Equation,” *Complexity*, Vol. 2022, No. 1, p. 2158052, Jan. 2022, doi: <https://doi.org/10.1155/2022/2158052>
- [42] T. S. Maughan *et al.*, “Comparison of intermittent and continuous palliative chemotherapy for advanced colorectal cancer: a multicentre randomised trial,” *The Lancet*, Vol. 361, No. 9356, pp. 457-464, Feb. 2003, doi: 10.1016/S0140-6736(03)12461-0
- [43] H.-P. Ren, Y. Yang, M. S. Baptista, and C. Grebogi, “Tumour chemotherapy strategy based on impulse control theory,” *Philosophical Transactions of the Royal Society A: Mathematical, Physical and Engineering Sciences*, Vol. 375, No. 2088, p. 20160221, Mar. 2017, doi: 10.1098/rsta.2016.0221
- [44] D. Zhao, N. Zhao, H. Zhang, P. Shi, and I. Rudas, “Resilient Sampled-Data Event-Triggered Control for Switched Systems Under Denial of Service Attacks,” *Acta Polytechnica Hungarica*, Vol. 21, No. 10, pp. 263-282, 2024
- [45] R.-C. Roman, R.-E. Precup, and E. M. Petriu, “Active Disturbance Rejection Control for 3D Crane Systems,” *Procedia Comput Sci*, Vol. 242, pp. 976-983, 2024, doi: <https://doi.org/10.1016/j.procs.2024.08.267>
-

- [46] A. Takacs, L. Kovacs, I. J. Rudas, R.-E. Precup, and T. Haidegger, "Models for Force Control in Telesurgical Robot Systems," *Acta Polytechnica Hungarica*, Vol. 12, No. 8, pp. 95-114, 2015
- [47] R.-C. Roman, R.-E. Precup, E. M. Petriu, and A.-I. Borlea, "Hybrid Data-Driven Active Disturbance Rejection Sliding Mode Control with Tower Crane Systems Validation," *Romanian Journal of Information Science and Technology*, Vol. 27, No. 1, pp. 50-64, 2024, doi: 10.59277/ROMJIST.2024.1.04
- [48] T. Haidegger, L. Kovács, R.-E. Precup, B. Benyó, Z. Benyó, and S. Preitl, "Simulation and control for telerobots in space medicine," *Acta Astronaut*, Vol. 81, No. 1, pp. 390-402, 2012, doi: <https://doi.org/10.1016/j.actaastro.2012.06.010>
- [49] I. A. Zamfirache, R.-E. Precup, and E. M. Petriu, "Adaptive reinforcement learning-based control using proximal policy optimization and slime mould algorithm with experimental tower crane system validation," *Appl Soft Comput*, Vol. 160, p. 111687, 2024, doi: <https://doi.org/10.1016/j.asoc.2024.111687>
- [50] T. Yang, *Impulsive Control Theory*. in Lecture Notes in Control and Information Sciences. Berlin, Heidelberg: Springer Berlin Heidelberg, 2001, doi: 10.1007/3-540-47710-1
- [51] B. Brogliato, "Impulsive Dynamics and Measure Differential Equations," in *Nonsmooth Mechanics: Models, Dynamics and Control*, B. Brogliato, Ed., Cham: Springer International Publishing, 2016, pp. 1-49, doi: 10.1007/978-3-319-28664-8_1
- [52] J. C. Butcher, "Numerical Differential Equation Methods," in *Numerical Methods for Ordinary Differential Equations*, John Wiley & Sons, Ltd, 2016, ch. 2, pp. 55-142, doi: <https://doi.org/10.1002/9781119121534.ch2>
- [53] MathWorks, "MATLAB Optimization Toolbox." [Online] Available: <https://www.mathworks.com/products/optimization.html>
- [54] Y. Nesterov and A. Nemirovskii, *Interior-Point Polynomial Algorithms in Convex Programming*. Society for Industrial and Applied Mathematics, 1994. doi: 10.1137/1.9781611970791
- [55] J. Nocedal and S. J. Wright, "Interior-Point Methods for Nonlinear Programming," in *Numerical Optimization*, New York, NY: Springer New York, 2006, pp. 563-597, doi: 10.1007/978-0-387-40065-5_19